Sedimentology (1986) **33**, 261–277

The record of density-induced underflows in a glacial lake

FRANK WEIRICH

Department of Geography, U.C.L.A., Los Angeles, CA 90024, U.S.A.

ABSTRACT

As part of an overall study of sedimentation processes in a proglacial lake an effort was made to compare field results with some of the general equations for density flows. The results suggest that in relatively small glacial lakes the occurrence of underflows with lower sediment loads involves a complex interplay between thermal and sediment effects which is extremely sensitive to varying hydrologic and climatic conditions. In terms of actual transport mechanics the results: (i) indicate that a higher α value of 0·6 or 0·7 gives a closer agreement between the measured velocity values and the established equations on moderately shallow slopes; (ii) provide field support for the experimentally derived relationship of Britter & Linden (1980) for the velocity of underflows and suggest the equation may be applicable in situations below 5° slopes; and (iii) support the relationship between velocity of the front and body of a continuous underflow for moderate slope situations suggested by Middleton (1966b). Finally the velocity values measured by electromagnetic current meters stationed in the lake, the grain-size data obtained from mapping core data, and the application of other criteria support the concept that in this environment the underflows are capable of erosion.

INTRODUCTION

Studies of the processes operating in glaciolacustrine environments have indicated that density, and in particular turbidity underflows, have an important role in sedimentation (Gilbert, 1973a, b; Gustavson, 1975; Lambert, Kelts & Marshall, 1976; Smith, 1978, 1981; Lambert & Hsü, 1979; Gilbert & Shaw, 1981). A similar conclusion has been reached by those who have studied glaciolacustrine deposits (e.g. De Geer, 1940; Banerjee, 1973; Gustavson, 1975; Theakstone, 1976; Shaw & Archer, 1978; Sturm & Matter, 1978). There has, however, been a lack of detailed field-based process data of such phenomena. This study was undertaken to further our understanding of density induced underflow processes in different environments. Specifically it sought to: (1) obtain detailed knowledge of the circumstances under which currents take place by means of a basin-wide hydrologic, climatologic and sedimentologic monitoring programme; and (2) also to monitor the subsurface movement of underflows in this environment using a three-dimensional sensor network.

THE STUDY SITE

The site selected for the study was the uppermost lake in a string of three situated in the Purcell Mountains of British Columbia at Latitude 51°N and Longitude 116°W. The location, topography and overall character of the site are provided in Figs 1, 2 and 3. A detailed discussion of the site characteristics has been given in Weirich (1982). What made this site particularly attractive to study, as a high energy glacial environment, was the setting which included:

(a) a relatively small, clearly definable sub-basin of some 6·5 km containing a single major ice mass feeding via a single stream into a small, shallow lake (mean depth 5 m) with a simple bottom character and a single outlet stream;
(b) a simple Gilbert type delta with only a small number of channels crossing its surface;
(c) the dominance of the glacier as the major source of both water and sediment for the lake;
(d) rapidly fluctuating input conditions;
(e) a straightforward geology with only one formation

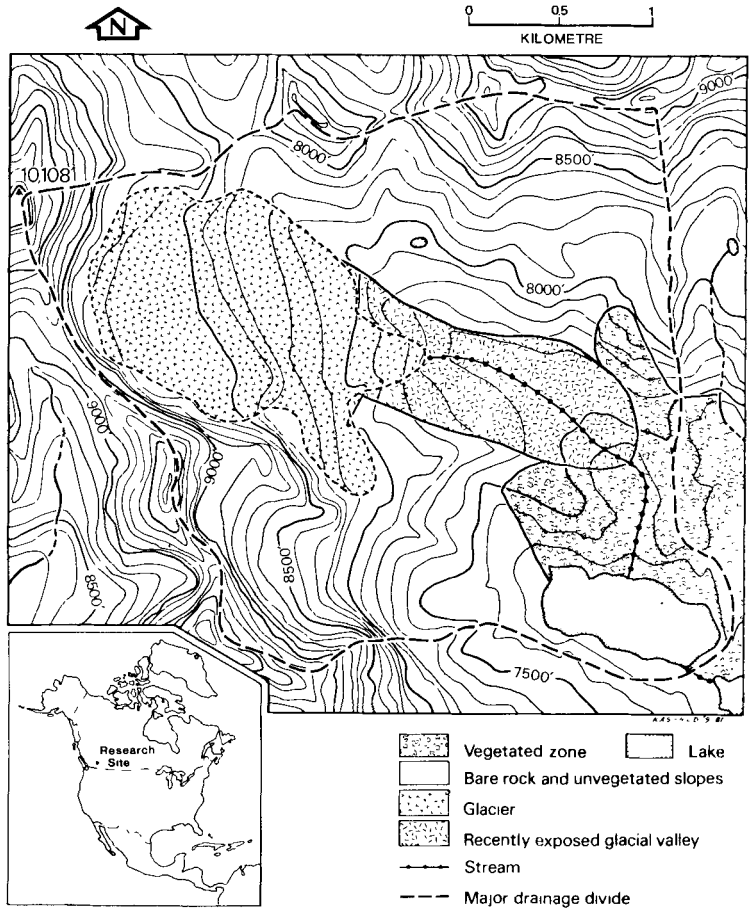

Fig. 1. Location, topography and physiographic units of the research site.

(the Mt Nelson Formation) dominating the sub-basin and serving as the major rock source for material entering the lake.

Overall, the site provided an uncomplicated field situation, a setting well-suited for a detailed process study of sedimentation in a high energy glacial environment.

INSTRUMENTATION

The effort to carry out monitoring of the occurrence and nature of density underflows was part of a broader basin-wide hydrologic, climatic, and sedimentological study. The work was initiated in the spring of 1976 and continued over the course of the following three years with continuous monitoring of processes taking place during the summer melt periods. A detailed discussion of the overall instrumentation aspects of the entire project has been presented in Weirich (1982). Of concern here is the underwater monitoring system used to detect and track the density underflows. The underwater system, shown in Fig. 4, consisted of a 3-D sensor network located in the area in front of the delta. It was comprised of nine stations with three sensor packages stacked vertically at each station for a total of 27 sensor locations. An aerial view of the network is provided in Fig. 5. Each of the 27 sensor packages in the grid consisted of: a precision temperature sensor measuring water temperature to 0·05°C; a photo-optical sensor consisting of a reference and measuring cell to monitor the suspended sediment concentration; and a remotely controlled bank of

Fig. 2. The research site. Water from the glacier (upper left of plate) is carried by a single meltwater stream which reaches the lake through a ravine cut into bedrock (the Mt Nelson Formation). The delta (in the centre of the photo) has several distributary channels crossing its surface. Lake level usually determines which of the channels will be active at a particular time. The outflow channel (seen in the foreground) is cut into bedrock and drains into a second lake some 100 m down valley.

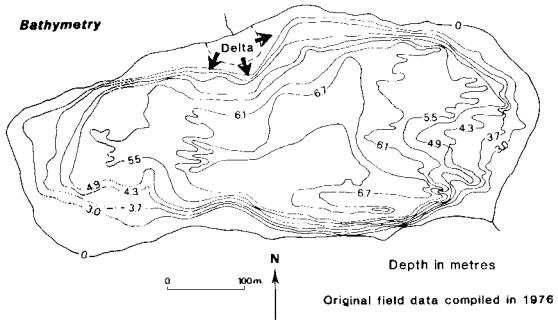

Fig. 3. As the bathymetric map indicates the lake floor is relatively uniform with a few shallow depressions extending toward the NW and northern areas. The arrows indicate the location of major surface stream channels crossing the delta and entering the lake.

samplers which was intended to provide *in situ* water and sediment samples to enable calibration of the optical sensor (see Fig. 6). The individual sensor packages were mounted in groups of three on aluminium frames in order to enable adjustment of both sensor package spacing and height above the lake bed. Each of the frames were anchored to the lake bed and to surface rafts. The location of these sensor stations could also be readily changed to adjust to changing conditions in the lake. In addition to the standard sensor packages, two Marsch McBirney electromagnetic current meters were operated in order to obtain direct measurements of the currents. These units, measuring velocity in both the X and Y directions simultaneously, were able to provide data on both low and higher velocity underflow events. Finally, a tenth station was established at mid-lake to supply reference levels for the main underwater sensor array as well as to provide data on lake conditions.

Information on input and output discharge was provided by Stevens A-71 water level recorders calibrated with an Ott current meter following conventional gauging procedures. A programme of water and sediment sampling at 08:00, 12:00, 16:00, 20:00, and when possible 23:00 each day, in conjunction with continuous monitoring of stream temperatures and turbidity, and the operation of both a valley and lake climate station provided additional data on changes in input and output conditions.

All continuous data (some 90 channels plus 30 channels of calibration and reference level data) were transmitted via cable to a shore based central instrument station overlooking the delta. A Flute Summa II data logger scanning at 15 channels s^{-1} with scan intervals ranging from 10 s up to 10 min was used to record the information on both paper output and on to magnetic tape using a Kennedy incremental tape recorder. Additionally, data were recorded on chart and multipoint recorders. Finally, stratigraphic data were obtained through a coring programme involving both manual and hammer driven coring systems operated from a specially modified 4·9 m aluminium boat equipped with a well-winch system (Weirich, 1982).

RECORD OF EVENTS

The data presented below are for one day, day 28 of the 1978 season (10 August 1978) and are illustrative of the type of data obtained. Figure 7 indicates the locations of the electromagnetic current meters and the optical network. Figure 8 presents electromagnetic current meter records for a morning underflow event. Figure 9 indicates an afternoon event. In both figures the X-axis represents the forward velocity and the Y-axis the downward flow as the underflow moves out and down the delta foreslope. The continuous underflow began at approximately 07:30 and continued until 11:30 when activity came to a rather abrupt end. The afternoon event was much shorter in duration, beginning at 14:07 and continuing for only some 10 min.

In addition to the current meter records both events were also detected by the 3-D underwater optical

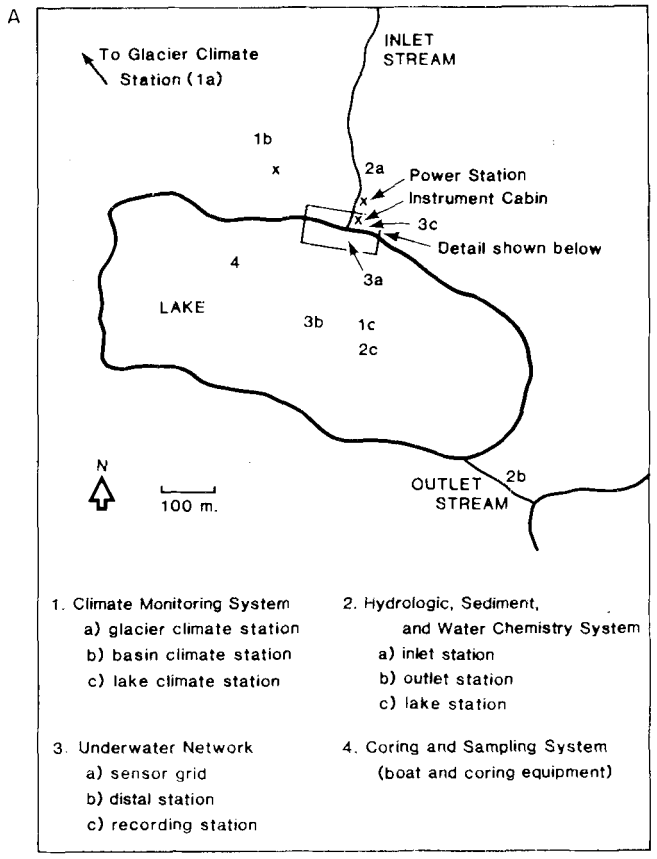

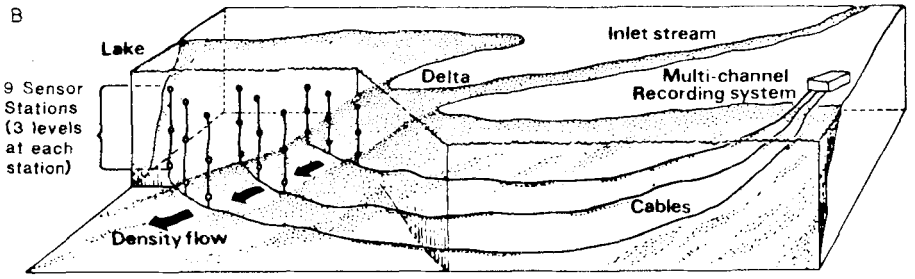

Fig. 4. (A) Location of major facilities. The instrument cabin contained the main recording facilities as well as a small laboratory and workshop. (B) The 3-D underwater network monitored the movement of currents into the lake. Information from the network was transmitted to the recording equipment in the instrument cabin through a series of trunk cables crossing the lake floor. Each of the nine monitoring stations consisted of a surface raft and three sensor packages suspended from anchors.

Fig. 5. An aerial view of the 3-D network in place. The individual stations were shifted about in order to adjust to changing input conditions. Small marker floats are also visible. They provided reference points for tracking the surface movement of the currents. The distal raft indicates the location of an electromagnetic current meter which was used to monitor movement beyond the grid.

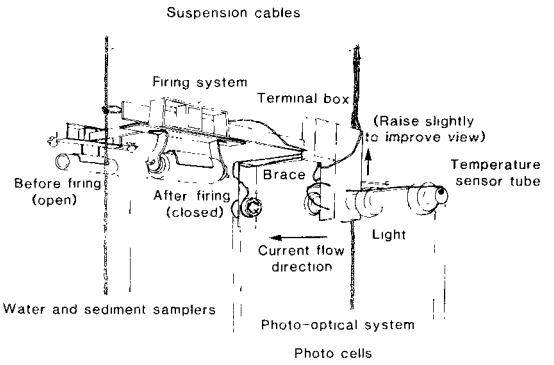

Fig. 6. The instrument package deployed within the underwater sensor network. The package contained: a sensitive thermistor for water temperature, a photo-optical sediment sensing system employing a measuring and reference cell system, and a set of solenoid operated, remotely controlled water samplers.

system. Figure 10 presents the optical sensor readings for each of the three sensor packages at L2S1 and at L2S3 on that day (see Fig. 7). In each of these figures, level 1 readings were taken at 1·5 m above the bed while level 2 and 3 readings were taken at 1·0 and 0·5 m respectively above the bed. The optical readings presented are background corrected values; that is, the lake values obtained from the tenth station situated at mid-lake have been subtracted from the original optical output values. The optical data given are in millivolts as a relative measure of sediment concentration. Laboratory calibration indicates that an approximate relationship exists with $1\ \text{mV} = 1\ \text{mg}\ \text{l}^{-1}$ sediment load concentration 10%.

The conditions under which these underflows took place are of interest. The week preceding these events was one in which there were no dramatic climatic or hydrologic changes. The total precipitation during this period amounted to less than 10 mm. Incoming solar radiation values during this time ranged from 59 to 70 MJ $\text{m}^{-2}\ \text{day}^{-1}$, and the mean air temperature remained at approximately 14°C with no rapid shifts beyond the normal diurnal variation (from approximately 0°C to 19°C) as periods of sun and scattered cloud persisted. The lake remained essentially isothermal during this time with the mean temperature remaining at 6°C.

Of particular interest are the meteorologic, hydrologic and sedimentologic conditions of the day of the events. The incoming solar radiation record for the day (presented in Fig. 11A) indicates a relatively cloud-free early morning with the rise to the maximum value of 850 W m^{-2} at 15:00 being interrupted by clouds in the early afternoon (from 12:00 to 14:00). Similarly, the peak period also saw a substantial drop in incoming radiation from 16:00 to 17:30 due to the presence of late afternoon cloud.

The record of input stream temperature (Fig. 11C) clearly reflects the effect of solar heating of the input water. From 00:00 to 05:00 the input stream temperature remained at 2·5°C. Following a slight drop between 06:00 and 07:30 it began a steady rise peaking initially at 7°C and subsequently at over 8°C at approximately 16:00 before declining throughout the afternoon and returning to a level of 2·5°C by 24:00. Of note are the two drops in temperature from 7·5 to 5·5°C and from 8·5 to 6·5°C. These drops correspond with the periods of reduced solar radiation.

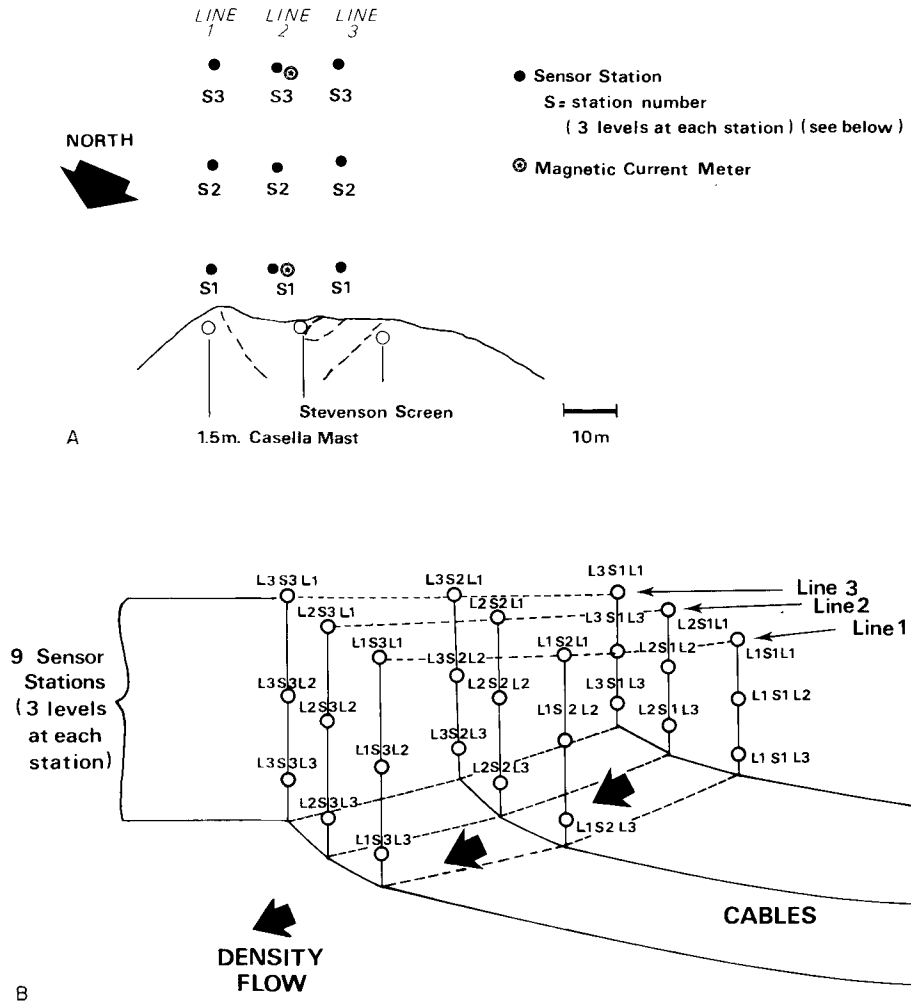

Fig. 7. The location of the underwater network. (A) A plan view of network showing the location of the nine sensor stations with respect to the delta and some of the delta surface instrumentation. The location of the electromagnetic current meters is also indicated. For the purposes of identification the 3-D network was divided into three lines and each station in a line numbered from the shore outward. Finally each sensor package was numbered as to its level at a station starting from the surface downward. The location of the stations could be shifted as needed to adjust to changing flow conditions. (B) Oblique view of the underwater network. Note the numbering scheme (line, station, level) used to identify each package in the network.

In contrast, the average lake temperature remained relatively stable throughout the entire day, ranging from 7·5°C to 8·0°C (Fig. 11C). Examination of lake temperature profiles show that isothermal conditions prevailed.

The discharge record for the incoming stream (Fig. 11C) does not reflect the input stream temperature pattern. Instead, the response is much more subdued with a gradual drop from 00:00 to 10:00 followed by a steady rise to the discharge levels at 18:00. The lateness of the peak appears to reflect not only the normal lag but also the effect of the late morning and mid-afternoon cloud periods. It should also be noted that no sudden changes in discharge occurred.

The record of sediment flux (Fig. 11D) is an interesting one. Starting from an initial concentration of 140 mg l^{-1} (consisting of both suspended and dissolved materials) the levels began a gradual rise

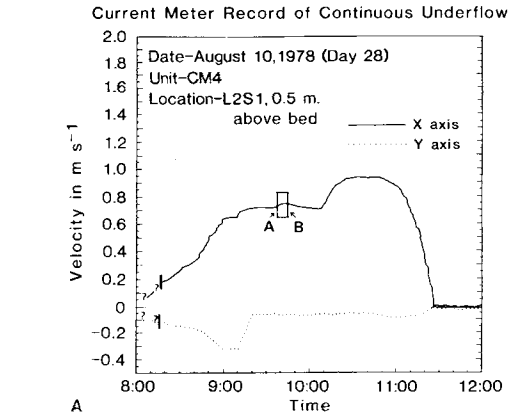

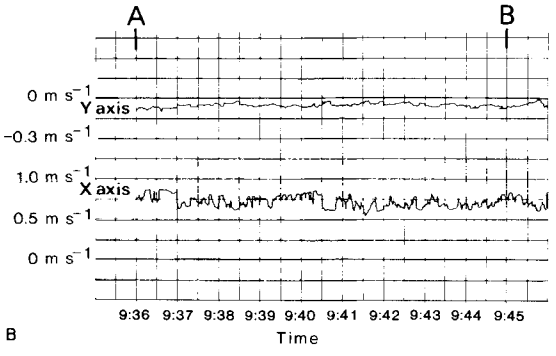

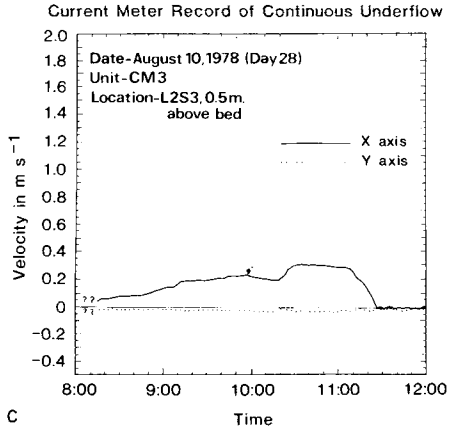

from 08:00 to 10:00, levelled off at 250 mg l^{-1} for some 4 hr before rising above 300 mg l^{-1} at 16:30 and declined gradually to return to a level of 140 mg l^{-1} by 20:00. The anomaly in this pattern is the brief but substantial rise to above 550 mg l^{-1} which occurred shortly after 14:00, a peak which does not correspond with any of the other input data variations. Mean combined dissolved and suspended sediment flux data from the lake throughout the day indicate steady levels with values ranging from 40 to 50 mg l^{-1}.

The combined effect of the hydrologic, climatic and sedimentologic factors is to produce variations in the density difference between the incoming stream waters and the waters of the lake. The density differences resulting from the effects of temperature and sediment (both dissolved and suspended) differences are presented in Fig. 12. The range in total density differences from $0{\cdot}8 \times 10^{-1}$ kg m^{-3} to $4{\cdot}5 \times 10^{-1}$ kg m^{-3} is of considerable significance. What is perhaps of more significance is the fact that this total density difference is clearly the result of a complex interplay between sediment and thermal fluxes.

The essentially stable temperature (2·5°C) and sediment load (150 mg l^{-1}) of the input stream from 00:00 to 07:00 produced a relatively stable density difference of $1{\cdot}6 \times 10^{-1}$ kg m^{-3}. Beginning at approximately 07:00 the rise in inlet temperature and sediment load produced a steady increase in the total density difference. Shortly after, at 08:00, the total density difference reached $1{\cdot}9 \times 10^{-1}$ kg m^{-3} and underflow began. While the rise in sediment load is significant in contributing to the density difference, it is the density difference resulting from the warming of the input stream that dominated the underflow process at this point (Fig. 12). During the subsequent three hours, the stream temperatures rose to 7°C. In doing so, the density difference between the input

Fig. 8. Electromagnetic current meter readings from the morning of 10 August 1978 at two different stations which document the occurrence of a continuous underflow lasting some 3·5 hr. (A) The $+X$-axis value is the velocity of the current in a lakeward horizontal direction, while the $-Y$-axis value is the bottomward vertical component of the flow as it moves out into the lake. (B) A detailed view of a small segment of the current meter record. A pulsing in the flow is present which does not correlate with any changing inflow conditions. Note that flow conditions were supercritical during this period. (C) A parallel record to that shown in (A) and (B) only this unit is located at another station some 40 m further lakeward of the first. Although velocities are considerably lower they exhibit the same general form as those of the shoreward unit.

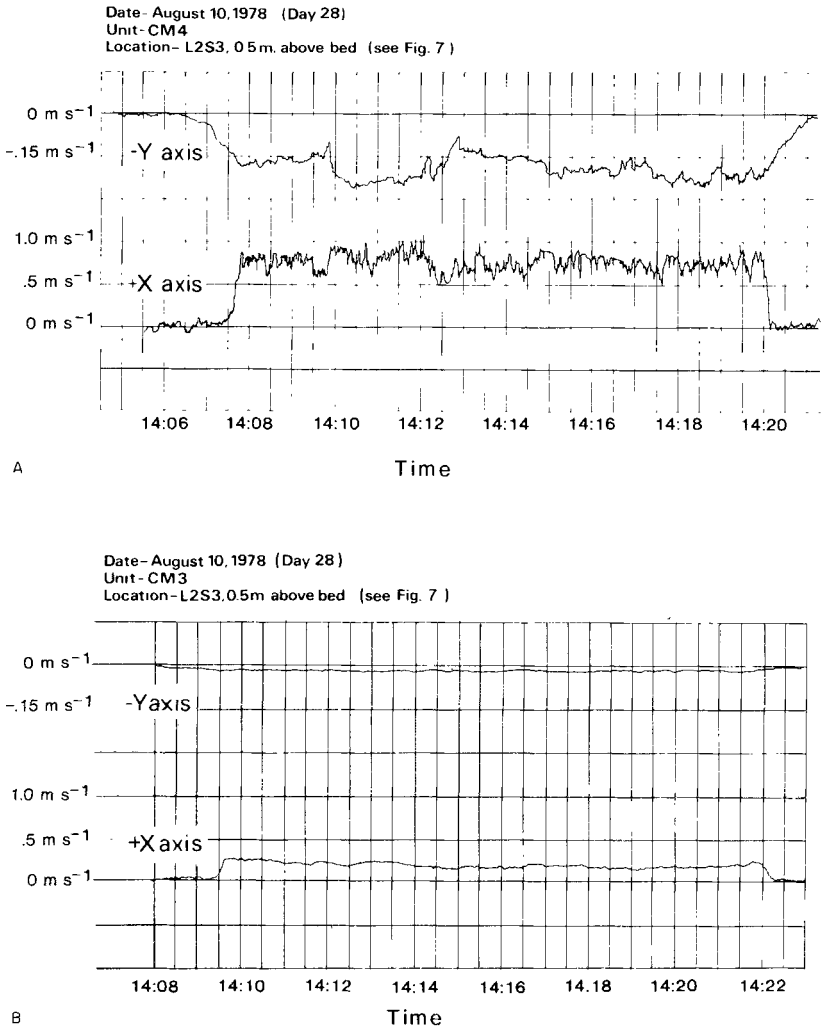

Fig. 9. The record of the day 28 afternoon event. The electromagnetic current meter record shows both X and Y velocities (see Fig. 8 caption for an explanation of axis orientation). (A) The record for a near shore location (L2S1; Fig. 7) shows a pulsing pattern and a very distinct initiation and termination signal with very little falling off or tail effect indicating that a single slug of material moved quickly through the system. As in the case of the morning event flow was supercritical and no input variations occurred which could account for the pulsations. (B) The event produced a much more subdued, but nevertheless consistent, response in the more distally located unit.

stream water and the lake water increased to a maximum value at approximately 10:00 when the input stream water temperature reached 4°C (at which point the incoming water would be at its maximum thermal density). As the input stream water continued to warm after 10:00 the density difference between input water and lake water began to decline. During the same three hour period the suspended load began a steady climb, reaching over 260 mg l^{-1} by 11:00. The underflow velocity peaked at 10:40 at 0·91 m s^{-1}. As the morning progressed and the input stream temperatures continued to rise to well above the 4·0°C thermal maximum density, the input water density decreased further and the total density difference declined. By 11:30, the total density difference between input and lake had dropped below

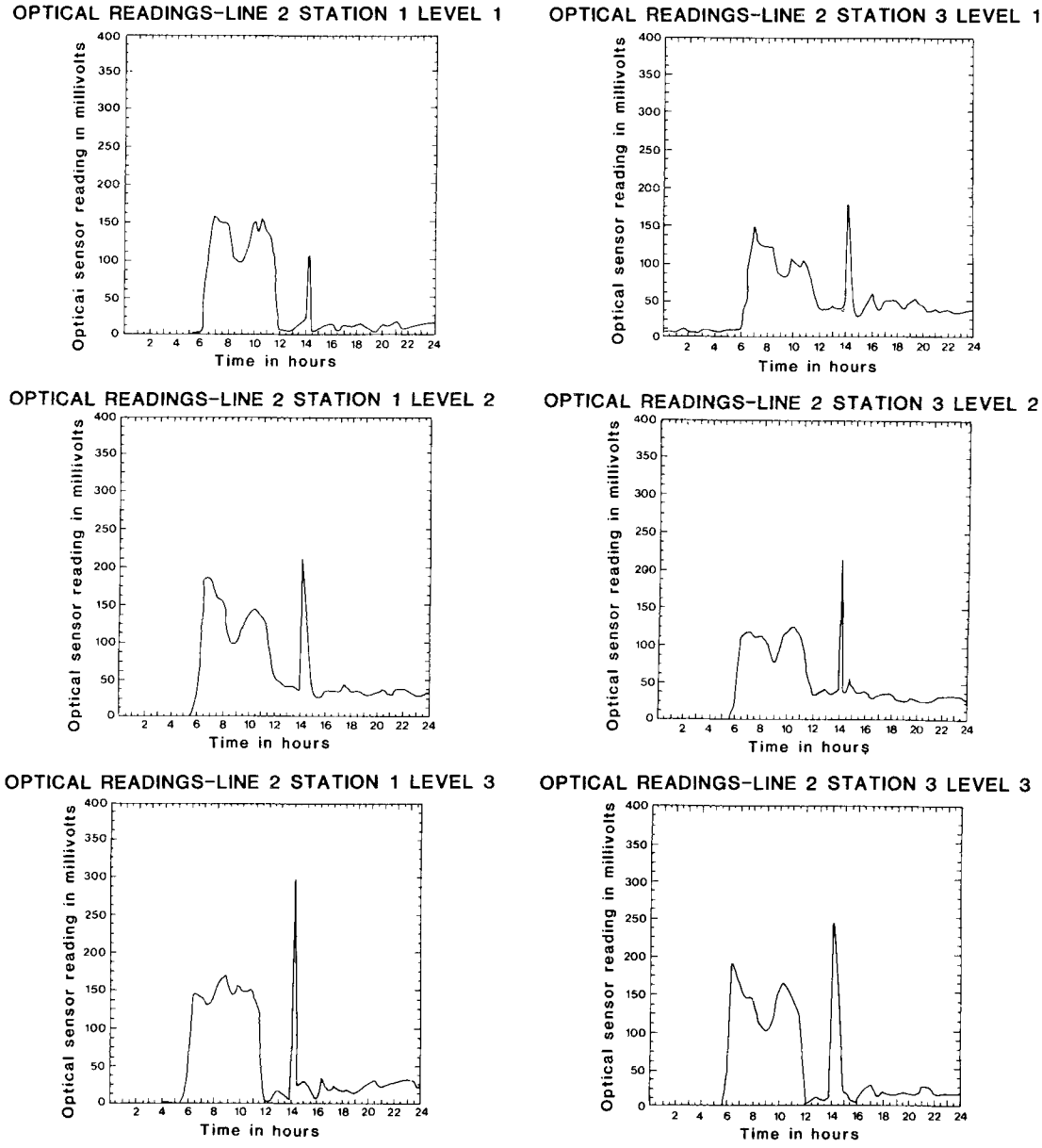

Fig. 10. Optical sensor readings for 10 August 1978 at two of the nine stations and at three levels for each of the stations. The readings reflect the relative concentrations of suspended sediment at specific points in the sensor grid and indicate the passage of an underflow lasting several hours in the morning and the occurrence of an afternoon surge event. Although there is considerable variation between the different levels the morning event showed little stratification within the flow while the afternoon event showed a marked stratification, especially at the shoreward location.

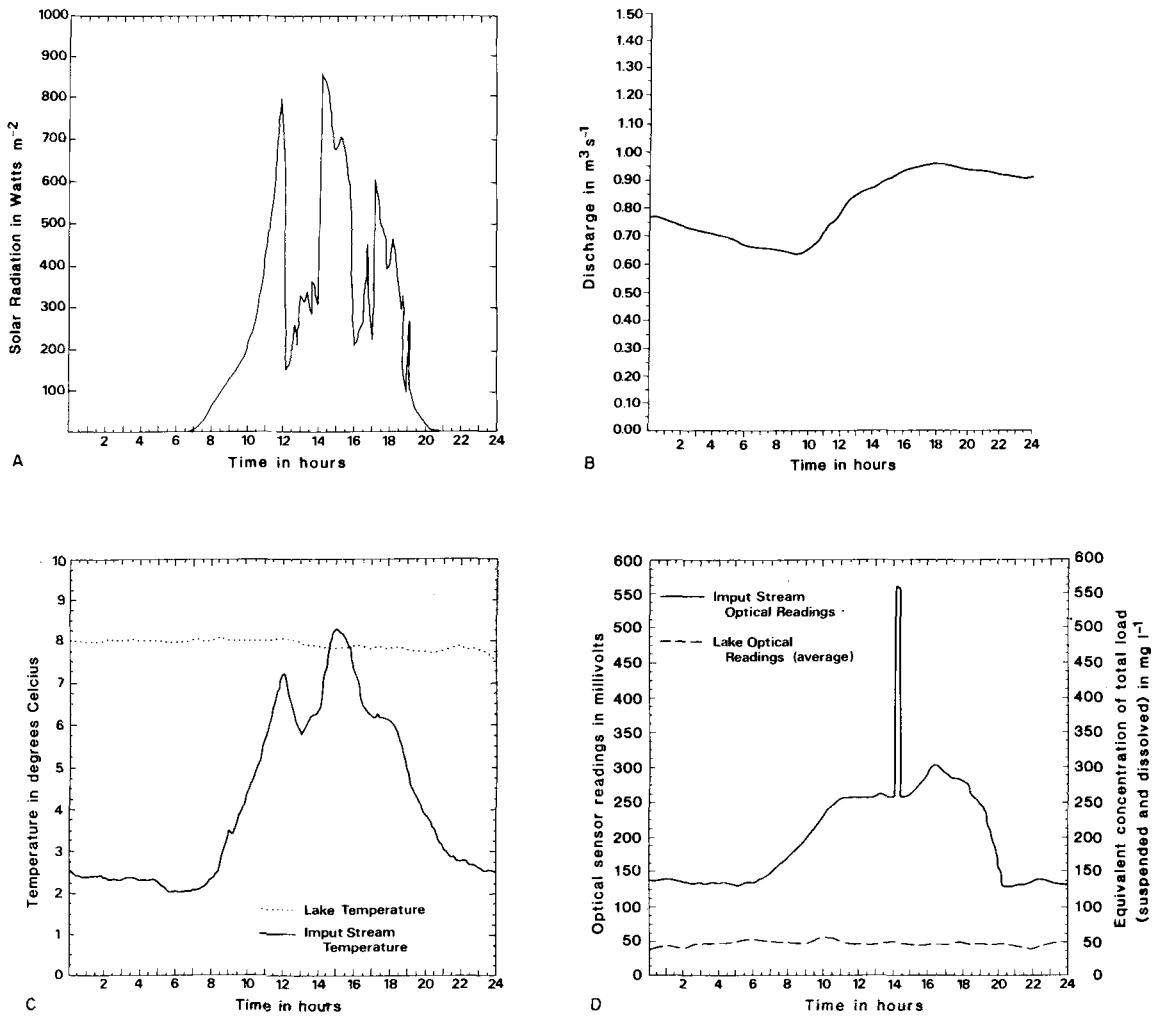

Fig. 11. (A) The solar radiation record for 10 August 1978 measured at the climate station some 300 m from the delta. (B) The input stream discharge record for the same day. (C) The input stream water temperature and lake temperature for the day. The stream temperature was measured on the delta surface only 10 m from where the water entered the lake to minimize any effects of temperature changes before the stream water entered the lake. The lake temperature was taken at a location beyond the sensor grid where there would be little effect from underflow currents. The value given is the mean for a profile taken at three different levels. (D) The input stream and lake total sediment loads. These are based upon optical sensor readings and analysis of discrete water samples which were used to calibrate the optical readings. As in the case of temperature values presented are the average of all sensors in the vertical profile string.

$1{\cdot}9 \times 10^{-1}$ kg m^{-3} and the underflow ended. Although the sediment load remained constant, the decreasing density of the warming input water had ended the underflow. The effect of solar heating of the input water is considerable. Comparison of the incoming solar radiation values (Fig. 11A) with the temperature of the incoming stream (Fig. 11C) and the thermally produced density differences between stream and lake indicates a close correlation (Fig. 12).

At 14:07 the second event began. Although there was no sudden change in discharge (Fig. 11B) or input stream temperature (Fig. 11C) there was a sudden increase in suspended load from 260 to 550 mg l^{-1} in less than one minute (Fig. 11D). The resulting turbidity

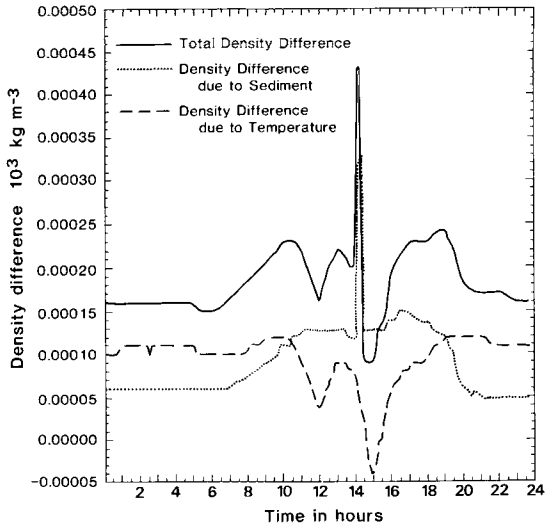

Fig. 12. The total density difference between the input stream water and the lake water showing the density difference contributed by the different components of suspended and dissolved sediment and thermally produced differences. The record indicates the initiation of both morning and afternoon underflows when the total density difference exceeded $1{\cdot}9 \times 10^{-1}$ kg m^{-3} and the cessation of the events when the levels dropped below that level. The occurrence of early evening underflow event is also indicated, however this was not confirmed by the sensor network. It is possible this evening event moved out via one of the other channels crossing the delta and hence was not in the flow path of the sensor network.

current reached a peak velocity of over 1·0 m s^{-1}. It then ended abruptly at about 14:20. Given that the suspended sediment increase was detected on the optical sensor located in the input stream, subaqueous slump initiation of this event may be ruled out. The most likely source of the sediment is from a slumping of material from the stream bank, possibly in the area immediately below the glacier snout where the stream dissects deposits of silts.

This event was not detected at any stations on line 1 of the optical system (see Fig. 7) or at stations 1 and 2 of line 3. It was, however, detected on all three stations of line 2 and at station 3 of line 3. The underflow moved out through the middle of the network and then appears to have spread out towards the right portion of the grid. Alternatively, the readings at station 3 of line 3 may have been the result of the presence of a concurrent density underflow moving out from one of the other delta stream channels.

Following the surge event, the suspended sediment concentration dropped rapidly to approximately 260 mg l^{-1}. The input stream continued warming and therefore dropped in density relative to the lake, reaching a peak temperature of 8·3°C at approximately 15:00. Subsequently, the input temperature dropped to 6·3°C (at 16:00) and this temperature drop was accompanied by an increase in sediment load to above 280 mg l^{-1}. The combined effect of lower input temperature (producing a higher density for the input stream), and the greater density due to the increased sediment load, resulted in another underflow which did not move through the underwater grid but instead apparantly emanated from one of the delta stream channels. It continued until 20:00 when decreasing sediment load ended the event (Fig. 12).

MECHANICS OF MOVEMENT

While the conditions under which underflows occur are of considerable interest the actual mechanics and movement pattern of these currents are also of concern. Our present understanding of the actual flow dynamics of such density induced underflows is drawn largely from laboratory, and to a lesser extent theoretically based studies of subaqueous density and turbidity underflows. From such theoretical and laboratory studies has emerged the recognition that underflows are similar, in many respects, to processes underway in most subaerial fluvial situations (Harleman, 1961). However, marked differences also exist, because, in addition to the interaction between the fluid and the bed, the interaction at the upper fluid interface also becomes significant (Middleton, 1966a, b). Such differences in interface conditions result in significant differences in the character of underflows. Beginning with Bell (1942) and continuing through more recent studies the fundamental distinction between density induced underflows and turbidity currents has also been established. In the case of the density induced underflows the density difference is produced by some combination of thermal, dissolved or suspended sediment components and characterized by the maintenance of a constant bouyant flux (A in Ellison & Turner, 1959). For turbidity currents the suspended sediment is the dominant source of the density difference and there is a tendency toward a varying bouyant flux (varying A in the terms of Ellison & Turner, 1959).

Underflows have also been further divided on the basis of flow characteristics into two broad categories:

surge type currents and continuous feeding underflows (Middleton, 1966a). The surge type underflows are usually linked to high initial sediment concentrations, and are often associated with slumping or other rapid disturbance situations, while the continuous feeding underflows are usually associated with lower concentration loads and somewhat more stable input of material by rivers and streams feeding into a body of water. In fact, however, more complex forms occur (Luthi, 1980). The head or front of an incipient underflow will be similar in many respects (although not entirely, see Britter & Linden, 1980) to a 'pure head' surge while the body of such a flow will have a continuous character. Laboratory and theoretical efforts have also led to the recognition that the character of both surge (discontinuous) and continuous underflows vary substantially under differing slope conditions (Britter & Linden, 1980; Beghin, Hopfinger & Britter, 1981) with a general distinction between higher (5°–90°) and low slopes (0°–0·5°) and the presence of some form of transition zone between these conditions (0·5°–5°) (Denton, Faust & Plate, 1981).

The majority of the studies of surge type events have been based upon laboratory studies of the flow of saline heads. Kuelegan (1957, 1958) suggested that for surge type events the velocity of the flow could be described by an equation of the form:

$$V = C_d \sqrt{(\Delta\rho/\rho_2)\, g\, d} \qquad (1)$$

where:

V = speed of head surge,
C_d = a drag coefficient,
g = acceleration due to gravity,
d = thickness of head current,
$\Delta\rho$ = difference in density between the head and and the ambient fluid,
ρ_2 = density of lower fluid.

In the case of his own experiments he found that as the surge left the lock the initial drag coefficient was 0·46 but as the underflow became established the drag coefficient increased to 0·70. Middleton (1966a) found general accord with Kuelegan's formulations and close agreement with the coefficient C_d which he calculated to be 0·44 and 0·75 for the initial and subsequent flow respectively. From experimental work under more varied laboratory conditions, Kersey & Hsü (1976) suggested that the coefficient C_d is not constant but varies with Re, the depth of the flow versus total fluid depth (d/h), the degree of slope and the magnitude of frictional energy losses.

Much of this work, however, has been confined to surges on relatively low slopes. More recently, Beghin *et al.* (1981), working on steeper slopes, suggested the following non-dimensional relationships for surge flows:

$$U_f/(g' Q_0/x_f)^{1/2} \simeq 2{\cdot}6\,(\pm 0{\cdot}2) \text{ at } 15° \text{ slope} \quad (\text{decreasing to} \simeq 1{\cdot}5 \pm 0{\cdot}2 \text{ at } 90° \text{ slope}), \qquad (2)$$

where:

U_f = the velocity of the head or front,
g' = the reduced gravitational acceleration $(\Delta\rho g/\rho_2)$ with g = gravity,
ρ = the driving density difference,
ρ_2 = fluid density,
Q_0 = discharge per unit width,
x_f = front position as measured from a virtual origin.

The second type of underflow, the continuous feeding underflow, is quite different in character from surge type events and demonstrates many of the features usually associated with steady flow processes. Harleman (1961) suggested the following equation (essentially a modified form of the Chezy equation) for the velocity of flow:

$$u = \sqrt{8\, g' \frac{ds}{f(1+\alpha)}} \qquad (3)$$

where:

u = mean velocity of underflow,
$g' = g\,(\Delta\rho/\rho_2)$ with g, $\Delta\rho$, ρ_2 as above,
d = thickness of underflow,
s = slope of bed,
f = Darcy friction factor,
$\alpha = \tau_i/\tau_0$ with τ_i = interface shear stress, τ_0 = bed shear stress.

Middleton (1966b), while also utilizing a modified form of the Chezy equation, employed a somewhat different approach in dealing with the calculation of the friction in which the bed friction (f_0) and the interface friction (f_i) are related to Re for smooth channels and is estimated for rough channels using a Moody diagram.

Middleton's experimental results, also laid heavy emphasis upon the role of the densiometric Froude number (Fr_d) as a principle control of f_i with:

$$Fr_d = \frac{u}{\sqrt{(\Delta\rho/\rho_2)\, g\, d}} \quad (4)$$

with $\bar{u}$, $\Delta\rho$, ρ_2, g, d as above.

Provided that $Fr < 1$ there will be relatively little mixing and a low value of f_i. As Fr increases, the relative significance of f_i also increases. Moreover, it has also been shown that as the slope increases the relative significance of f_i versus f_0 appears to increase (Middleton, 1966b; Luthi, 1980). This pattern persists on much steeper slopes as well. In fact, Turner (1973) has suggested that on steeper slopes bottom friction may be largely ignored as f_i becomes dominant. Britter & Linden (1980), on much steeper slopes have found a relatively simple relationship with:

$$u_f/(g'\, Q_0)^{1/3} = 1{\cdot}5\,(\pm\, 0{\cdot}2), \quad (5)$$

with U_f, g', Q_0 as above.

The densiometric Froude number is regarded as important in such continuous feeding flow situations not only in terms of the interface frictions but also with respect to the matter of hydraulic jumps. Komar (1971, 1975) and others (Hand, 1974, 1975) have suggested that hydraulic jumps may occur in turbidity currents, particularly at changes in slope. The resulting shift from supercritical to subcritical flow should be accompanied by an abrupt decrease in velocity and an increase in flow thickness.

Much effort has also been expended to determine the relationship between the head or front of incipient underflows and the main body of the flows. Britter & Linden's experimental work on density flows on steep slopes (5°–90°) suggests a stable relationship with ($U_f/\bar{u}$) of 0·6. Middleton (1966a) on lower angle slopes found that the ($U_f/\bar{u}$) may vary with the slope.

The availability of relevant field data to enable comparison with the models which have been established is limited to, at most, field information from one or two stations in the line of flow or multiple location but non-continuous, profile data. The 3-D network, in addition to detecting the occurrence of underflows, also provided a significantly more detailed record of the actual flows. This capability was enhanced by the small size of the lake and the simple delta form which, while somewhat limiting the scope of the investigation, in effect provided a natural outdoor laboratory in which to study the flows. A comparison of data from the network with the models was therefore undertaken.

Data from the network indicate that both the morning underflow and the afternoon event followed similar routes moving 20 m down a slope of 0·227, and then 40 m down a slope of 0·037 before moving out into the central portion of the lake (see Fig. 13). As shown in Figs 8 and 9, both events were also detected

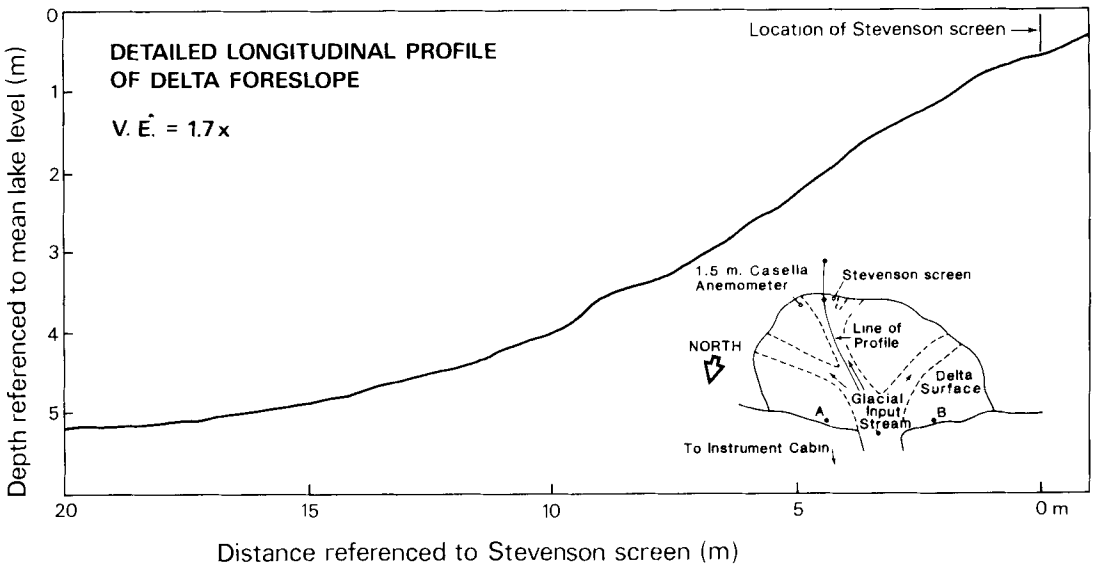

Fig. 13. Longitudinal profile of the input stream crossing the delta and reaching out into the lake along the line of the route followed by the underflows.

by each of the electromagnetic current meters, the first at line 2, station 1, halfway (10 m) down the initial steep slope, and the second electromagnetic unit at line 2, station 3, some 40 m beyond the first unit and 50 m from shore on the gentler slope.

The morning underflow began slowly with a gradual rise in density and accompanying velocity (see Figs 8 and 12). The peak velocity of 0·91 m s^{-1} was not reached until later in the morning when the density difference reached its maximum of $2{\cdot}5 \times 10^{-1}$ kg m^{-3}. During the early stages of the underflow, the $-Y$ (downward) component of the flow was relatively large (reaching 0·15 cm s^{-1}). Subsequently, the $-Y$ component decreased and stabilized, even as the X component was increasing. This anomalous situation may reflect the changing conditions at the plunge point. With relatively low density differences at the point of initiation of the underflow, the input flow would tend to move outward from the shore some distance and then sink, producing a relatively high $-Y$ component. As the density difference increased, the incoming water would tend to plunge at a point closer in to shore. As the flow moved away from the input point there was a substantial drop in velocity (from 0·91 m s^{-1} at the first current meter to only 28 m s^{-1} at the second). This may reflect not only the effect of changes in slope but also the likelihood that the flow conditions had not yet stabilized in the early portion of the flow and/or that the input stream was still affecting the current. The depth of the flow, as indicated by the optical sensor data, was at least 1·5 m (the height of the upper level sensors). Given the lack of visual surface evidence of the underflows (even in the relatively shallow areas of the foredelta beyond the plunge point), a reasonable estimate of the actual flow thickness on the steep slope might be 2–3 m or less. That the underflow probably did not thicken on the gentler slope further offshore is suggested by the maintenance of sediment concentration from station 1 to station 3 in both lines 2 and 3; thus, a similar value of 2–3 m flow depth seems reasonable. Calculation of the densiometric Froude (using the estimated depth 1·5–2·0 m, the measured density differences, and the velocity values of 0·20–0·90 m s^{-1} on the steep slope and 0·8–0·28 m s^{-1} on the shallow slope) indicate supercritical conditions on both the steep and shallow slope during the entire underflow event and hence no hydraulic jump occurred. The supercritical conditions may also account for the pulsations present in the flow velocity record.

The character of the afternoon surge event was somewhat different than the continuous underflow. Unlike the morning underflow, the surge underflow began rapidly reaching a velocity of 0·85 m s^{-1} within 1 min of onset and subsequently continued to increase reaching a peak value of 1·1 m s^{-1}. It then continued as a pulsating flow ranging from 0·75 to 1·1 m s^{-1} until the flow abruptly ended. As in the case of the morning event there was a rapid drop in velocity between the first and second current meters. The optical sensors indicated a flow depth of at least 1·5 m and the earlier estimate of 2–3 m for the flow depth may be applied to this event as well. The densiometric Froude (equation 4) was calculated using a $d = 2{\cdot}0$ m and a density difference of $4{\cdot}5 \times 10^{-1}$ kg m^{-3}. On both slopes the flow was supercritical and no hydraulic jump occurred. Unlike the situation of the continuous flow, however, the optical sensor system did indicate a clear stratification of the sediment in transport. Thus, the depth of flow at station 3 and the internal density variation within the flow are not known with the same level of assurance as in the case of the morning event. It is estimated that the flow depth was in the order of 2 m.

In order to compare these field results with the theoretical and experimental data it is necessary to make some assumptions regarding the character of the underflows. First, the approximately constant sediment concentrations indicated by the optical sensors as the flows move through the network suggests that the quantity of suspended particles which may be leaving the current (through sedimentation) or entering the current (through erosion) relative to the total amount of material suspended in the flows is relatively small. For comparison purposes therefore the flows may be treated as density currents with a constant bouyant flux (A in Ellison & Turner, 1959). Second, the presence of a shallow channel in the bed and the essentially uniform density distribution along the sensor line suggests that the underflows be treated as two dimensional rather than 3-D flows. Finally, a further distinction as to whether the flows are continuous or discontinuous (surges) is also needed. The duration of the morning event, and the gradual changes in conditions which occurred, would suggest that this event may be considered as a continuous feeding type of flow. The afternoon event has a more complex character. Beginning with an initial surge lasting only a short period of time, the main body of the flow continued for some 12 min. Rather than being considered as either a simple 'pure head' surge, a cloud-like thermal, or as only a continuous underflow, this event might be best described as an incipient underflow (Middleton, 1966b; Luthi, 1980) with a

surge-like front followed by a body of flow which will exhibit a more continuous character. The continuous classification of the main body of the flow is supported by: the relatively stable velocity of the flow over the 11 min period following the passage of the front; the duration of the event relative to the overall scale of the site; and the relatively stable sediment concentration over the flow period of the main body of the event. Thus the morning event may be treated as a continuous 2-D density underflow while the afternoon event may be characterized as a 2-D incipient underflow with a surge-like front or head and a continuous flow body (effectively a starting plume) (Britter & Linden, 1980).

Equation (5) was applied to the data available on the movement of the morning continuous overflow down the steep slope of the delta. Using a $\Delta\rho$ of $2{\cdot}5 \times 10^{-1}$ kg m^{-3}, $d = 2{\cdot}0$ m, $Q_0 = 1{\cdot}0$, and assuming a $U_f/\bar{u}$ of 0·6 (Britter & Linden, 1980) the equation yields a dimensionless expression of the velocity of 3·9. This is substantially higher than the value of 1·5 ($\pm 0{\cdot}2$) suggested by Britter & Linden (1980). This result supports the earlier suggestion that the flow has not yet stablized at this point. There is considerable likelihood that the incoming flow and developing underflow is still being affected by the subaerial incoming stream waters.

Both the Harleman equation (equation 3) and the Britter & Linden equation (5) were used to calculate flow velocities of the morning event on the shallow slope beyond the steep delta face. An f value of 0·010 was used (see Harleman, 1961 and Normark & Dickson, 1976). An α value of 0·43, based upon the findings of Harleman (1961) was used. Using a slope of 0·037, $d = 2{\cdot}0$ m, and a density difference of $2{\cdot}5 \times 10^{-1}$ kg m^{-3}, the calculated average velocity was 0·32 m s^{-1}. This was an overestimate compared with the measured velocity of 0·28 m s^{-1}. In addition, the average velocity of the underflow is likely to be even lower than the measured value of 0·28 m s^{-1} given the location of the current meter above the bed. The overestimation of velocity under these circumstances is not unexpected. Middleton (1966b) has shown that as Fr increases, f_i increases. Given the supercritical conditions present in this event, a more appropriate α value might be 0·6 or 0·7. Equation (5) was also employed to assess the flow of the current on the shallow 3·7% slope beyond the delta proper. The $\Delta\rho$ of $2{\cdot}5 \times 10^{-1}$ kg m^{-3}, $d = 2{\cdot}0$ m, and $Q_0 = 1{\cdot}0$, were utilized. With a $\bar{u}$ of 0·28 m s^{-1}, $U_f = 0{\cdot}19$ m s^{-1} was established (using a $U_f/\bar{u} = 0{\cdot}7$ for a slope of 3·7% following the findings of Middleton, 1966b). The non-dimensional result in terms of equation (5) yields a value of 1·4 which is well within the theoretical range suggested by the authors.

Equations (1), (3) and (5) were also applied to the afternoon event on the steep slope. Both equations (2) and (5) were used to calculate the velocity of the head of the afternoon flow. With a density difference of $4{\cdot}5 \times 10^{-1}$ kg m^{-3}, $d = 2{\cdot}0$ m, $Q_0 = 1{\cdot}0$, $x_f = 10$ m and a U_f of 0·66 m s^{-1}, equation (2) gave a value of 31·4. Britter & Linden's equation (equation 5) with Q_0 again being 1·0, $\Delta\rho = 4{\cdot}5 \times 10^{-1}$ kg m^{-3}, and a measured U_f of 0·66 m s^{-1}, yielded a non-dimensional value of 3·92. As in the case of the morning event it would appear reasonable to suggest that these unusually high values reflect the still persistent effect of the incoming surface stream flow.

On the shallow slope equations (1), (3) and (5) were employed. The velocity of the front of the incipient underflow was evaluated using equation (1). Using a C_d of 0·75, a $\Delta\rho$ of $4{\cdot}5 \times 10^{-1}$ kg m^{-3}, and $d = 2{\cdot}0$ m, the estimated velocity was 0·07 m s^{-1} as opposed to the measured U_f value of 0·22 m s^{-1}. Using equation (5), with $Q_0 = 1{\cdot}0$, $p = 4{\cdot}5 \times 10^{-1}$ kg m^{-3}, $U_f = 0{\cdot}22$, gave a non-dimensional value of 1·3. The velocity of the body of the flow was evaluated using equations (3) and (5). Harleman's equation (equation 3) resulted in a calculated value of 0·43 m s^{-1}. This overestimated the measured value of 0·36 m s^{-1}. The outcome is consistent with the results obtained for the shallow slope flow of the morning event using the same equation. When Britter & Linden's equation (5) is utilized with the above data and applying the $U_f/\bar{u}$ proportionality of 0·7 for a slope of 3·7% (based upon Middleton's presentation of experimental data, see Middleton, 1966a), this yields a value of 0·36 m s^{-1}—a good agreement with the measured values.

THE STRATIGRAPHIC RECORD

Beyond the sensor grid, the character of the underflows is less certain. Analysis of data from some 150 cores taken from the lake bottom, however, provide further indirect information. The cores, averaging 0·5 m in length, were obtained using both manually pushed and hammer driven corers operating through a well installed in the floor of a 4·3 m aluminium boat. Both on-site extraction, examination and sampling as well as storage and return of a large number of complete cores was undertaken. The analysis of the cores involving grain-size determination and the examination of structures in the cores is discussed in more

detail in Weirich (1985). Attempts to detect changes in the transport processes by tracing horizontal variation in individual laminae were not successful. The relatively low mean sedimentation rates (of the order of 1·5 mm yr^{-1}) and the presence of substantial disturbance in the cores, especially in areas of frequent turbidity current activity, effectively prevented efforts to trace the presence of individual laminae continuously over any substantial distance. Grain-size data do, however, provide some useful information indicating both the occurrence and intensity of underflows. First, the presence of sand-size (over 4 phi) material in many of the cores, material with a settling rate in excess of $2{\cdot}5 \times 10^{-3}$ m s^{-1} is considered strong evidence of underflow activity. Moreover, in several of the distal cores, material of 0 phi size, with a settling velocity of 0·16 m s^{-1} were found. Applying Bagnold's criteria for autosuspension indicates that a velocity of 0·28 m s^{-1} would be required to transport material of this size to the present locations of these deposits (Normark & Dickson, 1976). A current with such a velocity and transporting material of such a size should also be capable of eroding channels (Hjulstrom, 1935; Sundborg, 1956).

DISCUSSION

Other studies dealing with underflows have tended to concentrate on high sediment load situations where the dominant factor in controlling the underflow process has clearly been variations in the sediment carried by the incoming stream. The results obtained in this study of processes underway in a small, relatively shallow, glacial lake, suggest that in lower sediment load situations, a complex interplay between thermal and sediment effects occurs. This points to the sensitivity of such events to changes in input and lake characteristics brought about by changing hydrologic and climatic conditions.

In terms of the actual transport mechanics, the largely thermally controlled continuous underflow of the morning is similar to the afternoon sediment controlled surge event. The major differences between the two, aside from the obvious difference in initiation conditions, is the presence of stratification of sediment in the afternoon event and the relatively uniform distribution of material in the morning continuous flow event. Comparison of the measured velocity values for both events with the established equations indicates: (i) the persistence of entrance effects in delta areas may limit the applicability of many flow equations; (ii) in the shallower slope areas ($\simeq 3°$), beyond the delta itself, a higher α value of 0·6–0·7 seems more appropriate; (iii) Britter & Linden's non-dimensional relationship of the velocity to other flow parameters $(U_f/g\ Q_0)^{1/3} = 1{\cdot}5\ (+0{\cdot}2)$ appears to hold both for the higher slope situation as well as below the lower (5°) slope limit found in their experimental work. The $U_f/u = 0{\cdot}7$ ratio for the afternoon event on the shallow slope also supports the experimentally determined portionality between the velocity of the front and the main flow of an incipient underflow ($U_f/\bar{u}$) discussed by Middleton (1966a).

The stratigraphic data indicate that density underflow activity is common in this environment. Moreover, the apparent frequency and extent of features characteristic of underflows suggests that underflows at various times and in various ways are involved in the transport of a substantial portion of the sediment in the lake. The stratigraphic evidence, in terms of grain-size parameters and the hydraulic criteria for transport of materials, also suggests underflow velocities have been operating on the floor of the lake in the past which are comparable to the values measured by the current meters in the network. Both the current meter velocities and the velocities derived from analysis of the stratigraphic data are sufficient to enable erosion by the currents.

ACKNOWLEDGMENTS

This work was initially funded by grants from the Canadian Federal Department of Energy, Mines, and Resources and the Canadian N.S.E.R.C. The loan of equipment by D. C. Ford, J. A. Davies, and W. Rouse of the Department of Geography at McMaster University; B. Goodison of the Canadian Atmospheric Environment Service; the Environmental Institute of the University of Toronto is gratefully acknowledged. The support and encouragement of A. V. Jopling of the Department of Geography at the University of Toronto was crucial to the conduct of this work.

Detailed computer and data analysis was carried out through the assistance of the Department of Geography, U.C.L.A. and computer and Academic Senate Grants from U.C.L.A. Cartographic work was ably carried out by Noel Diaz and Dirk Hanson of the Department of Geography, U.C.L.A.

REFERENCES

BANERJEE, I. (1973) Sedimentology of Pleistocene glacial varves in Ontario, Canada. *Bull. geol. Soc. Can.* **226**, 60 pp.

BEGHIN, P., HOPFINGER, E.J. & BRITTER, R.E. (1981) Gravitational convection from instantaneous sources on inclined boundaries. *J. Fluid Mech.* **107**, 407–422.

BELL, H.S. (1942) Density currents as agents for transporting sediments. *J. Geol.* **50**, 512–547.

BRITTER, R.E. & LINDEN, P.F. (1980) The motion of the front of a gravity current travelling down an incline. *J. Fluid Mech.* **99**, 531–543.

DE GEER, G. (1940) Geochronology suecica principles. *Kgl. Svenska Vetenskapskad. Handl.* **18** (6), 367 pp.

DENTON, R.A., FAUST, K.M. & PLATE, E.J. (1981) Aspects of stratified flow in man-made reservoirs. *SFB 80, Univ. Karlsruhe, Res. Rep. ET/203.*

ELLISON, T.H. & TURNER, J.S. (1959) Turbulent entrainment in stratified flows. *J. Fluid Mech.* **6**, 423–448.

GILBERT, R. (1973a) *Observations of lacustrine sedimentation in Lilooet Lake, British Columbia.* Unpublished Ph.D. thesis, University of British Columbia.

GILBERT, R. (1973b) Processes of underflow and sediment transport in a British Columbia mountain lake. In: *Fluvial Processes and Sedimentation, Proc. ninth Can. Hydrologic Symp.*, NRCC, 493–507.

GILBERT, R. & SHAW, J. (1981) Sedimentation in proglacial Sunwapta Lake, Alberta. *Can. J. Earth Sci.* **12**, 1697–1711.

GUSTAVSON, T.C. (1975) Sedimentation and physical limnology in proglacial Malaspina Lake, Southeastern Alaska. In: *Glaciofluvial and Glaciolacustrine Sedimentation* (Ed. by A. V. Jopling and B. C. McDonald). *Spec. Publ. Soc. econ. Paleont. Miner. No. 23.*

HAND, B.M. (1974) Supercritical flow in density currents. *J. sedim. Petrol.* **44**, 637–648.

HAND, B.M. (1975) Supercritical flow in density currents: reply. *J. sedim. Petrol.* **45**, 750–753.

HARLEMAN, D.R.F. (1961) Stratified flow. In: *Handbook of Fluid Dynamics* (Ed. by U. L. Streeter), McGraw-Hill, New York.

HJULSTROM, F. (1935) The morphological activity of rivers as illustrated by River Fyris. *Bull. geol. Inst. Uppsala*, **25**, CH III.

KERSEY, D.G. & HSÜ, J.K. (1976) Energy relations of density-current flows: an experimental investigation. *Sedimentology*, **23**, 761–789.

KOMAR, P.D. (1971) Hydraulic jumps in turbidity currents. *Bull. geol. Soc. Am.* **82**, 1477–1487.

KOMAR, P.D. (1975) Supercritical flow in density currents: a discussion. *J. sedim. Petrol.* **45**, 747–749.

KUELEGAN, G.H. (1957) Thirteenth progress report on model laws for density currents. An experimental study of the motion of saline water from locks into fresh water channels. *Rep. U.S. Natn. Bureau Stand., 5168.*

KEULEGAN, G.H. (1958) Twelfth progress report on model laws for density currents. The motion of saline fronts in still water. *Rep. U.S. Natn. Bureau Stand., 5831.*

LAMBERT, A. & HSÜ, K.J. (1979) Non-annual cycles of varve-like sedimentation in Walensee, Switzerland. *Sedimentology*, **26**, 453–461.

LAMBERT, A.M., KELTS, K.R. & MARSHALL, N.F. (1976) Measurements of density underflows from Walensee, Switzerland. *Sedimentology*, **23**, 87–105.

LUTHI, S. (1980) Some new aspects of two-dimensional turbidity currents. *Sedimentology*, **28**, 97–105.

MIDDLETON, G.V. (1966a) Experiments on density and turbidity currents I. Motion of the head. *Can. J. Earth Sci.*, **3**, 523.

MIDDLETON, G.V. (1966b) Experiments on density and turbidity currents II. Uniform flow of density currents. *Can. J. Earth Sci.* **3**, 627–637.

NORMARK, W.R. & DICKSON, F.H. (1976) Man-made turbidity currents in Lake Superior. *Sedimentology*, **23**, 815–831.

SHAW, J. & ARCHER, J. (1978) Winter turbidity current deposits in Late Pleistocene glaciolacustrine varves, Okanagan Valley, B.C., Canada. *Boreas*, **7**, 123–130.

SMITH, N.D. (1978) Sedimentation processes and patterns: in a glacierfed lake with low sediment input. *Can. J. Earth Sci.* **15**, 741–756.

STURM, M. & MATTER, A. (1978) Turbidities and varves in Lake Brienz (Switzerland): deposition of clastic detritus by density currents. In: *Modern and Ancient Lake Sediments* (Ed. by A. Matter and M. E. Tucker). *Spec. Publ. int. Ass. Sediment.* **2**, 147–168. Blackwell Scientific Publications, Oxford.

SUNDBORG, A. (1956) The river Klaralven, a study of fluvial processes. *Geog. Annlr.* **38**, 127–316.

THEAKSTONE, W.H. (1976) Glacial lake sedimentation, Austerdalsisen, Norway. *Sedimentology*, **23**, 815–831.

TURNER, J.S. (1973) *Bouyancy Effects in Fluids.* Cambridge University Press, 367 pp.

WEIRICH, F.H. (1982) Site locations and instrumentation aspects of a study of sedimentation processes in a proglacial lake in southeastern British Columbia, Canada. In: *Research in Glacial, Glacio-fluvial, and Glacio-lacustrine Systems, Proc. 6th Guelph Symp. Geomorphology*, 1980 (Ed. by R. Davidson-Arnott, W. Nickling and B. D. Fahey). Geo Books, Norwich, pp. 239–260.

WEIRICH, F.H. (1985) Sediment budget for a high energy glacial lake. *Geog. Annlr.* **67A** (1–2), 83–99.

(Manuscript received 29 November 1983; revision received 10 June 1985)